ELSEVIER

Thin Solid Films 398–399 (2001) 331–335

thin Solid films

www.elsevier.com/locate/tsf

On the measurement of stress–strain curves by spherical indentation

E.G. Herbert[a,b,*], G.M. Pharr[c], W.C. Oliver[d], B.N. Lucas[e], J.L. Hay[d]

[a]*MTS Nano Instruments Innovation Center, Oak Ridge, TN, USA*
[b]*The University of Tennessee, Knoxville, TN, USA*
[c]*University of Tennessee and ORNL, Knoxville, TN, USA*
[d]*MTS Nano Instruments Innovation Center, Oak Ridge, TN, USA*
[e]*Fast Forward Devices, Knoxville, TN, USA*

Abstract

It has been proposed that with the appropriate models, instrumented indentation test (IIT) data can be reduced to yield the uniaxial stress–strain behavior of the test material. However, very little work has been done to directly compare the results from uniaxial tension and spherical indentation experiments. In this work, indentation and uniaxial tension experiments have been performed on the aluminum alloy 6061-T6. The purpose of these experiments was to specifically explore the accuracy with which the analytical models can be applied to IIT data to predict the uniaxial stress–strain behavior of the aluminum alloy. Despite not being able to reproduce the physical shape of the uniaxial stress–strain curve, the results do indicate that spherical indentation can be successfully used to establish an engineering estimate of the elastic modulus and yield strength of 6061-T6. © 2001 Elsevier Science B.V. All rights reserved.

Keywords: Nanoindentation; Spherical; Indentation; Stress and strain measurements

1. Introduction

The primary objective of this work was to compare the stress–strain curve of the aluminum alloy 6061-T6 as determined by spherical indentation and uniaxial tension. To accomplish that goal, existing indentation models were used to develop what we felt to be the most appropriate indentation test method. Developing the most appropriate load–time algorithm and the most accurate and meaningful way to establish the point of contact and the instrument load frame stiffness were among the most critical aspects of building the test method. Each of these issues plays a critical role in obtaining the most precise and accurate mechanical property measurements possible.

Developing the test method was an iterative process. The final verification of the models and our test method was based on their ability to determine the elastic modulus of the standard reference material, which in this case was fused silica. Young's modulus was chosen to benchmark the models and test method performance because it is an intrinsic material property and, as indicated by Eqs. (5)–(9), it is a direct verification of whether or not the models and test method are calculating the correct contact area.

Once the models and test method demonstrated the ability to correctly measure the elastic modulus of the standard reference material, they were applied to the aluminum alloy 6061-T6. The primary questions were, can the models and test method accurately and precisely determine Young's modulus, E, and the yield strength, σ_y?

2. Theory

The models chosen to reduce the indentation data were that of Hertz [1], Oliver and Pharr [2] and Tabor [3]. Hertz's analysis, despite being based on the assumption of paraboloids in elastic contact, was chosen over

* Corresponding author. Tel.: +1-865-481-8452; fax: +1-865-481-8455.
E-mail addresses: blucas@ffdevices.com (B.N. Lucas), erik.herbert@mts.com (E.G. Herbert), pharr@utk.edu (G.M. Pharr), warren.oliver@mts.com (W.C. Oliver).

PII: S0040-6090(01)01439-0

Sneddon's [4] specific solution of spheres in elastic contact for two reasons: in the limit of small displacements ($2h_cR \gg h_c^2$), Hertz's solution is very similar to Sneddon's and Hertz's solution is algebraically much more simple. Hertz's analysis provides three expressions that are used in this investigation. First is the simple relationship between the total displacement into the sample, h, and the contact depth, h_c,

$$h = 2h_c \tag{1}$$

This is one expression among three that will later be used to indicate the yield point. Second is the following relationship between the load, P, and the contact radius, a,

$$P = \frac{4E_r a^3}{3R} \tag{2}$$

where E_r is the reduced or indentation modulus and R is the nominal radius of the indenter tip. Third is Hertz's relationship between the total displacement into the sample and contact radius,

$$h = a^2/R \tag{3}$$

Combining Eqs. (1)–(3), the relationship between load and contact depth can be simplified to

$$P = \frac{8\sqrt{2}}{3} E_r \sqrt{R} h_c^{3/2} \tag{4}$$

The importance of this expression is twofold. First, it provides a meaningful way to establish the point of contact and secondly it can be used to indicate when yielding has occurred.

Encompassed within the Oliver–Pharr model is the work of Pharr et al. [5], who showed that for all axisymmetric indenters, there is a constant relationship between the elastic contact stiffness, S, the projected area of contact, A, and the reduced or indentation modulus. The relationship is,

$$E_r = \frac{\sqrt{\pi}}{2} \frac{s}{\sqrt{A}} \tag{5}$$

In this context, the area is simply computed from the radius of the contact,

$$A = \pi a^2 \tag{6}$$

which is calculated from the following expression,

$$a = \sqrt{2h_cR - h_c^2} \tag{7}$$

The contact depth is established from the Oliver–Pharr model,

$$h_c = h - \varepsilon P/S \tag{8}$$

where h is the total measured displacement into the sample, and ε is a geometric constant based on indenter geometry; ε is 0.75 for a sphere. Furthermore, E_r is related to the elastic modulus of the sample, E_s, through the elastic modulus of the indenter, E_i, and Poisson's ratio of the indenter, ν_i, and the sample, ν_s:

$$E_r = \left[\frac{1-\nu_i}{E_i} + \frac{1-\nu_s}{E_s} \right]^{-1} \tag{9}$$

Therefore, given that we directly measure the contact stiffness, the only way to correctly calculate the known Young's modulus, E or E_s, is to calculate the correct contact area. It is important to note the contact area is determined only by the nominal radius of the indenter tip and the contact depth. There is no empirically derived 'area function' associated with the contact area calculation.

Three important observations of Tabor's [3] are also used in this analysis. First is the observation that yielding occurs when the mean pressure divided by the yield strength is approximately equal to 1.07,

$$p_m/\sigma_y \approx 1.07 \tag{10}$$

The next two observations of Tabor's go hand-in-hand. The true-stress and true-strain as determined from uniaxial tension data are equivalent to indentation stress and strain through the following two expressions:

$$\sigma_{\text{indentation}} \approx p_m/3 \approx \sigma_{\text{uniaxial tension}} \tag{11}$$

$$\varepsilon_{\text{indentation}} \approx 0.2a/R \approx \varepsilon_{\text{uniaxial tension}} \tag{12}$$

It is important to note that Eqs. (11) and (12) only hold true in the limit of a fully developed plastic contact. Based on the recent finite element investigations of Mesarovic and Fleck [6], this regime occurs when $a/R \approx 0.16$, independent of the magnitude of the non-dimensional parameters σ_y/E_r and Poisson's ratio.

3. Experimental methods

The indentation experiments were performed using a Nano Indenter® XP with MTS' continuous stiffness measurement (CSM) technique. With this technique, each indent gives the load, displacement, and contact stiffness as a continuous function of the indenter's displacement into the sample [2]. Loading was controlled such that the loading rate divided by the load was held constant at 0.05/s. Experiments were terminated at the maximum load of the standard XP head, approximately 70 g. The four spherical tips were single-crystal sapphire with diameters of 120, 200, 260 and 300 μm. The tensile experiments were conducted on an MTS 10/GL load frame with a 10 000-lb load cell. The dog bone samples were pulled at a rate of 0.05 mm/s.

4. Results and discussion

Fig. 1 represents the elastic modulus as a continuous function of the indenter's displacement into the sample

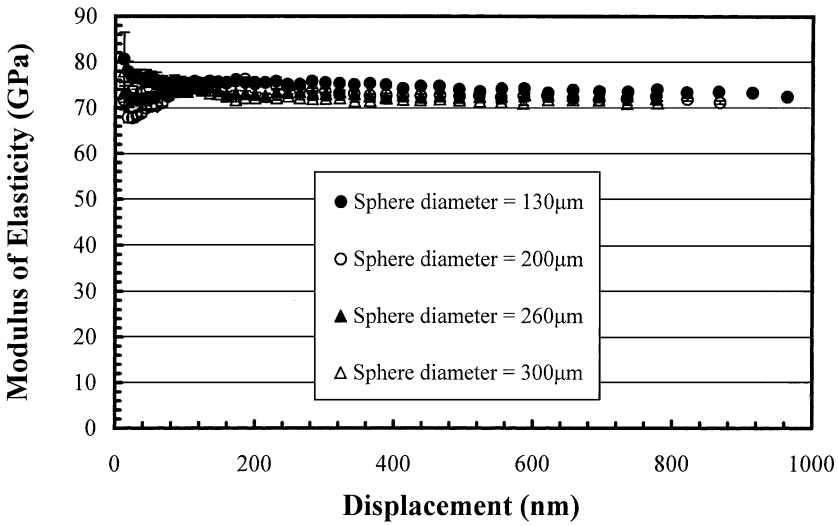

Fig. 1. Fused silica, modulus of elasticity as a function of the indenter's displacement into the sample.

for the standard reference material, fused silica. The literature value for fused silica is 72 GPa. Clearly, the models and method are doing a reasonably good job of evaluating the correct contact area using just the contact depth and the nominal radius of the tip. It is worth noting that all of the data in Fig. 1 are representative of an elastic contact, indicating that the Oliver–Pharr model simply reduces to Hertz's solution in the limit of an elastic contact. Furthermore, the silica data conformed very well to Eq. (1); the contact depth is indeed equal to one-half the total measured displacement into the sample.

Based on the ability of models and the test method to successfully determine the elastic modulus of the standard reference material, the next step was to apply them to the 6061-T6. Fig. 2 represents the elastic modulus as a function of the indenter's displacement into the sample for the 6061-T6. The average modulus value obtained from the tensile experiments was 70.09 ± 0.6 GPa. The literature value is 70.1 GPa. With modulus values obtained from indentation ranging from 67 to 75 GPa, the models and test method appear to be doing a reasonably good job of determining the elastic modulus. Furthermore, it is worth pointing out that the data in Fig. 2 are representative of elastic, elastic–plastic and fully developed plasticity, thereby providing solid testimony that the Oliver–Pharr model works well in all three regimes.

The next parameter of interest is the yield strength. Which promptly brings about the question, 'exactly how can we estimate when the sample has yielded?' Three different methods were explored in this work, all of

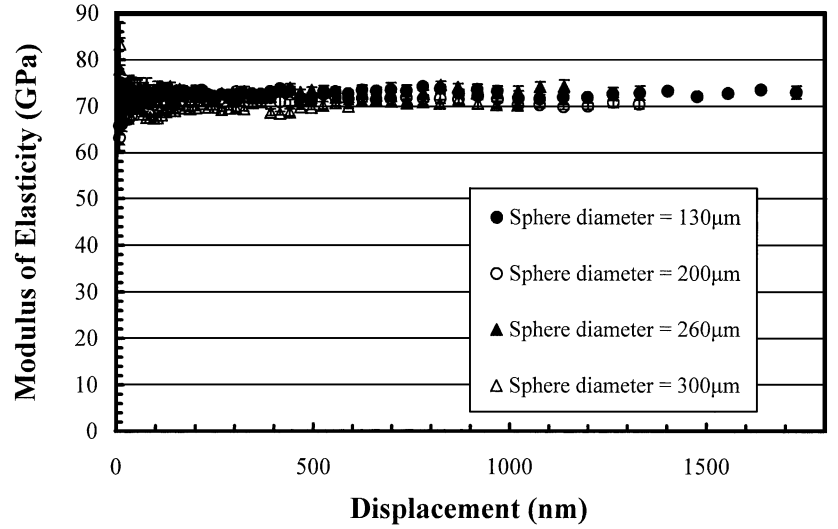

Fig. 2. 6061-T6, modulus of elasticity as a function of the indenter's displacement into the sample.

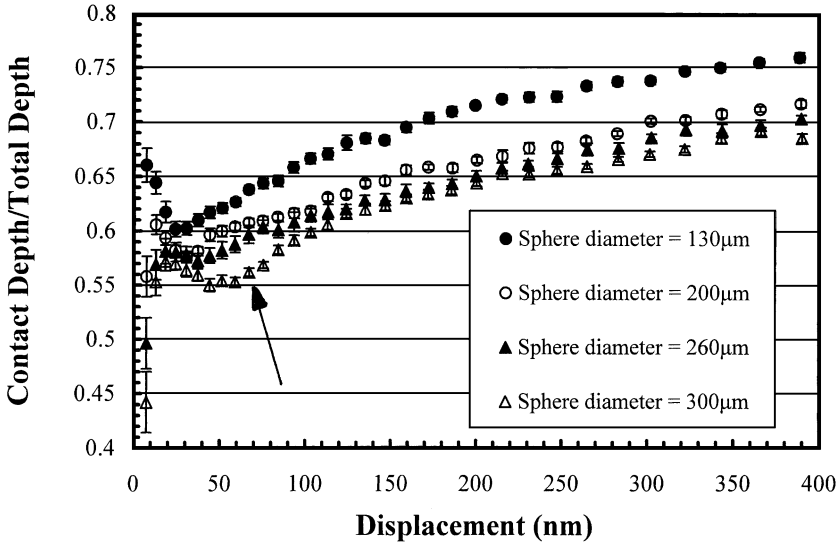

Fig. 3. 6061-T6, h_c/h as a function of the indenter's displacement into the sample.

which rely on a deviation from the expected elastic behavior predicted by Hertz. The three expressions used were as follows:

1. $h_c/h = 0.5$;
2. in the limit of small displacements $(2h_cR \gg h_c^2)$, $\frac{P^{2/3}}{\left((8\sqrt{2}/3)E_r\sqrt{R}\right)^{2/3}h_c}$; and
3. loading slope/unloading slope = 1.

All three relationships are known to hold true in the limit of an elastic contact. The yield point should be identifiable by any deviation from any one or all three expressions. Unfortunately, all three were equally poor performers in terms of providing any conclusive evidence of the yield point. In comparing the three, the ratio of contact depth to total depth arguably made the clearest distinction. Fig. 3 represents that ratio as a function of the indenter's displacement into the sample. Regrettably, the data do not provide any conclusive evidence of the yield point. As indicated by Hertz's analysis, the data for all four spheres should be constant at 0.5 until the material yields. As illustrated by Fig. 3, the data somewhat resembles that description but clearly at shallow depths it is not meeting expectations. Sorting out exactly what is causing these unexpected results will be an integral part of future work. Nevertheless, in an effort to make due with the acquired data, we chose to pick what we thought represented an upper and lower limit on the displacement at which yielding had occurred. In looking at the data from 400 nm towards the origin, for all four spheres, there is a distinctive curved shape that terminates at a small plateau or inflection point. With some confidence, the upper displacement limit for yielding was chosen to be the second-to-last data point that could be considered as part of that curved shape. For the 300-μm sphere, the upper limit is illustrated by the arrow in Fig. 3. Given justifiable concern as to whether or not the contact was ever solely elastic, choosing the lower displacement limit with any measure of confidence was deemed virtually impossible. Lacking a better alternative, the lower displacement limit for yielding was simply chosen to be the data point immediately left of the upper displacement limit. From the upper and lower limits, a yield strength range was calculated using Tabor's [3] observation that at the point of yielding, the yield strength is approximately equal to the mean pressure divided by 1.07 (Eq. (10)),

$$\frac{P/\pi a^2}{1.07} \approx \sigma_y \tag{13}$$

Plugging in the corresponding upper and lower limits for a led to the following average estimates of the yield strength:

- Lower limit: 399 ± 44.5 MPa.
- Upper limit: 426 ± 36.4 MPa.

The average result from the uniaxial tension experiments was 274 ± 2.3 MPa. The literature value is 276 MPa. The lower and upper estimates of the yield strength from the indentation data are 45 and 54% too high, respectively. Based on the ambiguity of method used to determine the yield point, these results are not too surprising.

Interestingly enough, however, the experimental results are very well corroborated by the recent finite element investigations of Mesarovic and Fleck [6]. Their results indicate that while yielding does occur at the point $p_m/\sigma_y \approx 1.07$, the first evidence of yielding does not actually occur until $p_m/\sigma_y \approx 1.6$. Using their 1.6 as

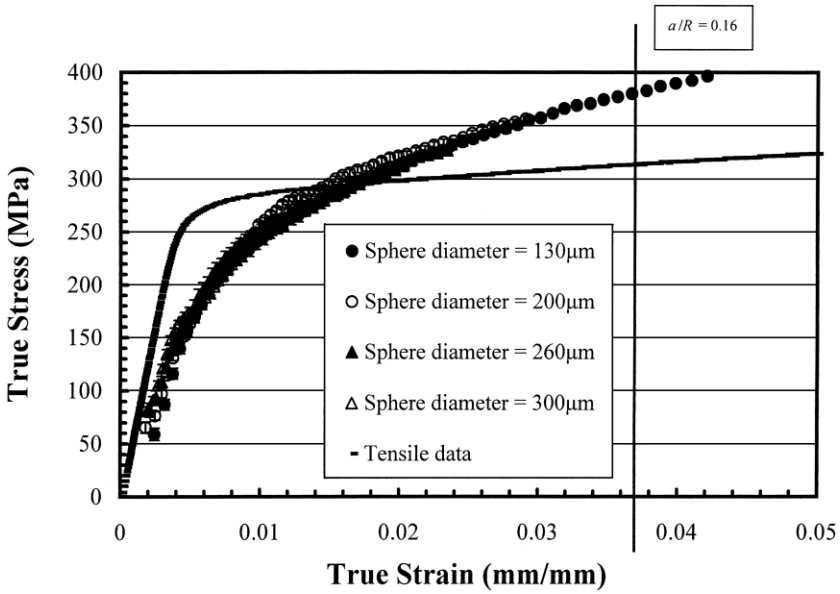

Fig. 4. The true-stress true-strain behavior of 6061-T6 as determined by uniaxial tension and spherical indentation.

opposed to 1.07 brings the lower and upper estimates of the yield strength to within −3.1 and 3.3% of the literature value, respectively.

Fig. 4 presents the true-stress true-strain curve for the aluminum alloy 6061-T6 as determined by uniaxial tension and spherical indentation. The vertical line through the plot indicates the point at which Tabor's observations, Eqs. (11) and (12), hold true. The line's position is representative of the point at which $a/R=$ 0.16. Although the indentation data to the left of the line does resemble the shape of a stress–strain curve, current indentation models in the literature do not provide any relationship between stress and strain in this regime.

5. Conclusions

With the correct models and careful attention to experimental detail, spherical indentation can be successfully used to determine the elastic modulus of 6061-T6.

With sphere diameters of 120, 200, 260 and 300 μm, a good engineering estimate of the yield strength of 6061-T6 can be made.

Applying Hertz's elastic models to spherical indentation data can be successfully accomplished in the limit of small displacements and truly spherical tip geometry.

With respect to 6061-T6 and fused silica, the Oliver–Pharr model has successfully demonstrated its ability to accurately predict the contact depth in all three indentation regimes: elastic, elastic–plastic, and fully developed plasticity.

References

[1] H. Hertz, in: H. Hertz (Ed.), Miscellaneous Papers, Jones and Schott, Macmillan, London, 1863.
[2] W.C. Oliver, G.M. Pharr, J. Mater. Res. 7 (6) (1992) 1564–1583.
[3] D. Tabor, Hardness of Metals, Clarendon Press, Oxford, 1951.
[4] I.N. Sneddon, Int. J. Eng. Sci. 3 (1965) 47.
[5] G.M. Pharr, W.C. Oliver, F.R. Brotzen, J. Mater. Res. 7 (1992) 613.
[6] S.D. Mesarovic, N.A. Fleck, Spherical indentation of elastic–plastic solids, Proc. Royal Soc. Lond. 455 (1999) 2707–2728.